Research Article

Journal of PeptideScience

Received: 20 October 2016 Revised: 5 January 2017 Accepted: 10 January 2017 Published online in Wiley Online Library

(wileyonlinelibrary.com) DOI 10.1002/psc.2974

Molecular design and synthesis of novel peptides from amphibians skin acting as inhibitors of cholinesterase enzymes

Alvaro Siano,[a] Francisco F. Garibotto,[b] Sebastian A. Andujar,[b]* Hector A. Baldoni,[c] Georgina G. Tonarelli[a] and Ricardo D. Enriz[b]

Cholinesterases are a family of enzymes that catalyze the hydrolysis of neurotransmitter acetylcholine. There are two types of cholinesterases, acetylcholinesterase (AChE) and butyrylcholinesterase (BChE), which differ in their distribution in the body. Currently, cholinesterase inhibitors (ChEI) represent the treatment of choice for Alzheimer's disease (AD). In this paper, we report the synthesis and inhibitory effect on both enzymes of four new peptides structurally related to P1-Hp-1971 (amphibian skin peptide found in our previous work. Sequence: TKPTLLGLPLGAGPAAGPGKR-NH_2). The bioassay data and cytotoxicity test show that some of the compounds possess a significant AChE and BChE inhibition and no toxic effect. The present work demonstrates that diminution of the size of the original peptide could potentially result in new compounds with significant cholinesterase inhibition activity, although it appears that there is an optimal size for the sequence. We also conducted an exhaustive molecular modeling study to better understand the mechanism of action of these compounds by combining docking techniques with molecular dynamics simulations on BChE. This is the first report about amphibian peptides and the second one of natural peptides with ChE inhibitory activity. Copyright © 2017 European Peptide Society and John Wiley & Sons, Ltd.

Additional supporting information may be found in the online version of this article at the publisher's web site.

Keywords: acetylcholinesterase; butyrylcholinesterase; peptide; docking; molecular dynamics

Introduction

Cholinesterases are a family of enzymes that catalyze the hydrolysis of neurotransmitter acetylcholine (ACh), an essential reaction necessary to allow a cholinergic neuron to return to the resting state after impulse transmission. There are two types of cholinesterases, i.e. acetylcholinesterase (AChE) and butyrylcholinesterase (BChE), which differ in their distribution in the body. AChE mainly exists in neuromuscular junctions and cholinergic synapses and hydrolyzes ACh with extremely high efficiency [1]. BChE is known as plasma cholinesterase, which is widely distributed in tissues and plasma. Although the physiological roles of BChE are still not completely clear, it has been known that BChE can catalyze the hydrolysis of various acyl cholines, acyl thiocholines [2], cocaine [3], and acetanilides [4]. It has been noted that BChE can rapidly hydrolyze ACh in the nerves and brain [5,6], and thus, BChE can apparently substitute for AChE in maintaining the structural and functional integrity of the central cholinergic pathway.

Currently, cholinesterase inhibitors (ChEI) represent the treatment of choice for Alzheimer's disease (AD), as shown by clinical studies on the effects of these drugs on cognition (memory and concentration) and also on behavioral symptoms (apathy and motor agitation). Noteworthy, AChE activity increases progressively in certain brain regions from mild to severe stages of AD to reach 10–15% of normal values, while BChE activity is unchanged or even increased by 20%, therefore a large pool of BChE is available in glia neurons and neuritic plaques [1]. It may not be an advantage for a ChEI to be selective for AChE; on the contrary, a good balance between AChE and BChE may result in higher efficacy [7].

Dementia is a syndrome characterized by impaired cognitive function beyond what might be considered a consequence of normal aging. Alzheimer's disease is the most common form of dementia: It is calculated that it represents between 60% and 70% of the cases [8]. The principle pathological hallmarks of the disease are senile plaques that consist of amyloid β and neurofibrillary tangles. The formation of these plaques in the hippocampal cholinergic neurons results in neuronal cell death via apoptotic pathway [9]. In view of the fact that most of the AD symptoms were related

* *Correspondence to: Sebastian Andujar, Facultad de Química, Bioquímica y Farmacia, Instituto Multidisciplinario de Investigaciones Biológicas (IMIBIO-SL. CONICET), Universidad Nacional de San Luis, Chacabuco 915, 5700 San Luis, Argentina. E-mail: saanduja@unsl.edu.ar*

a *Departamento de Química Orgánica, Facultad de Bioquímica y Cs. Biológicas (FBCB), Universidad Nacional del Litoral (UNL), Ciudad Universitaria, 3000, Santa Fe, Argentina*

b *Facultad de Química, Bioquímica y Farmacia, Instituto Multidisciplinario de Investigaciones Biológicas (IMIBIO-SL. CONICET), Universidad Nacional de San Luis, Chacabuco 915, 5700, San Luis, Argentina*

c *Facultad de Química, Bioquímica y Farmacia, Instituto de Matemática Aplicada San Luis, Universidad Nacional de San Luis (UNSL, CONICET), Ejército de Los Andes 950, 5700, San Luis, Argentina*

to loss of cholinergic function in the basal forebrain, cholinergic hypothesis was developed [10].

Moreover, the role of BChE in progression of AD has been proved. Furthermore, BChE inhibitors could recover cholinergic activity through restoring the AChE/BChE activity ratios as seen in a healthy brain [11]. As a result, investigations have been focused on dual AChE/BChE inhibitors [12].

Current approaches to the treatment of AD are the development of small molecule that inhibits proteases (secretases) which generate the β-amyloid peptide and also in the design of molecules that prevent the aggregation of this peptide [13]. While there is currently no cure for this disease, new drugs have been develop that can temporarily improve symptoms or slow the progression of this disease; ChEI such as Donepezil, Rivastigmine, and Galantamine are used.

As a result of research with some animal poisons, some toxins with anticholinesterase activity have been reported. The first reference to a toxin with this activity is melittin, a small polypeptide of 26 amino acid residues, isolated from the venom of *Apis mellifera* (European Bee), initially known for its hemolytic activity. The fasciculins (FAS) I and II, two polypeptides that inhibit both AChE and BChE, were isolated from the vemon of *Dendroaspisangusticeps* (green mamba) [14,15].

It has been previously reported in the literature different compounds with inhibitory properties of BChE. Among others, Donepezil, Galantamine, Cimserine, and Rivastigmine have displayed inhibitory activities against BChE [16–19]. Our own research group has recently reported a new alkaloid obtained from natural sources possessing a significant inhibitory effect on BChE [20]. However, peptide structures with significant inhibitory effects on this important enzyme have not been reported so far. In order to find new peptides that may have this effect, we performed an exploratory study by blind docking simulations in several and different peptides we had in our laboratory. In our previous work, we have reported that the extract of *Hypsiboas pulchellus* has inhibitory effect against BChE [21]. **P1-Hp-1971** is a proline–glycine and glycine-rich peptide with a random conformation who was previously isolated by our group from the skin of *Hypsiboas pulchellus*. Our preliminary study suggested that a proline–glycine-rich peptide (**P1-Hp-1971**, in Table 1) could act by an umbrella-type effect on the so-called gorge-butyryl site. In our previous work [21], we reported that this peptide possesses a highly random conformation and inhibits the growth of two ATCC strains: *Escherichia coli* (MIC: 16 μM) and *Staphylococcus aureus* (MIC: 8 μM). From all the peptides reported in that paper, **P1-Hp-1971** showed the highest Therapeutic Index (40 μM for *E. coli* and 80 μM for *S. aureus)*. Based on our preliminary results, we take the **P1-Hp-1971** as the initial structure, and we conducted a molecular modeling study in order to find new structurally related peptides possessing inhibitory effect against BChE. On the basis of these results, we have considered this peptide as an interesting initial structure for our study. Thus, in this paper, we report the synthesis and inhibitory effect on BChE of four new peptides structurally related to **P1-Hp-1971**. We also conducted an exhaustive molecular modeling study by combining docking techniques with Molecular Dynamics (MD) simulations to better understand the mechanism of action of these compounds. Besides FAS I and FAS II, there are no reports about other peptides that inhibit cholinesterase activity; furthermore, this is the first report about amphibian peptides and the second one of natural peptides with cholinesterase inhibitory activity.

Table 1. Sequences and properties of the synthetic peptides

Peptide	Region	Sequence	Nr	Molecular mass (Da)[a]	Net charge at pH = 7
P1-Hp-1971	—	TKPTLLGLPLGAGP AAGPGKR-NH_2	21	1971.173	+4
5–21	5–21	LLGLPLGAG PAAGPGKR-NH_2	17	1543.881	+3
7–21	7–21	GLPLGAG PAAGPGKR-NH_2	15	1317.565	+3
8–16	8–16	LPLGAGPAA-NH_2	9	764.923	+1
11–16	11–16	GAGPAA-NH_2	6	441.493	+1

All the peptides are amidated at their C-terminus. Purity >90%.
[a]Determined by Maldi-Tof.

Materials and Methods

Peptide synthesis

Peptides were synthesized (Table 1) as C-terminal amides by Fmoc solid-phase peptide synthesis using H-Rink Amide-Chem Matrix resin (Sigma). Couplings of 50 min were performed by *N*-[(1*H*–benzotriazol-1-yl)(dimethylamino)methylene]-*N*-methylmethanaminium hexafluorophosphate*N*-oxide and diisopropylethylamine**.** Fmoc removal was performed with 20% piperidine in DMF (*v*/v) (three times of 1 min each). Final cleavage from the resin was achieved by a mixture of TFA/H_2O/EDT/TIS (94.5 : 2.5 : 2.5 : 0.5) (*v*/v). After 3 h, the resin was filtered off, and the crude peptide was precipitated in dry cold diethyl ether, centrifuged, and washed several times with cold diethyl ether until the scavengers were removed. The product was then dissolved in water and lyophilized twice.

Set-up of the BChE

Starting coordinates were taken from the crystallographic structure of the recombinant and truncated human BChE at 2.0 Å resolution (PDB ID code: 1P0M) [22,23]. To build up our model of the native form of BChE, the following molecular fragments, present in the crystallographic model, were removed: five carbohydrate chains corresponding to five of the six expected glycosylation sites, three molecules of glycerol (used as a cryoprotectant), two sulfate ions, one molecule of 2-(*N*-morpholino)-ethanesulfonic acid, two chloride ions, and a butyrate molecule close to the catalytic Ser198 residue. In the crystal structure, coordinates were not available for residues 1–3, 378–379, and 455 owing to the lack of observed density. Residues 1–3 were omitted from our simulations, whereas the initial geometries for the residues 378–379 and 455 were modeled using the coordinates of *Torpedo californica* AChE as a template (PDB ID code: 1EA5) using Swiss model [24–26].

Docking of Peptides Compounds into the BChE

Docking calculations were carried out on BChE protein model (PDB ID code: 1P0M using the program high ambiguity-driven protein–protein docking (HADDOCK)) [27]. This program was also used to optimize the complex obtained (Webserver:http://haddock.science.uu.nl/services/HADDOCK/haddock.php). The 'targeted' molecular docking was performed using the following active site residues: W82, E325, S198, F329, E325, and H438.

Default HADDOCK parameters were used. Obtained docking solutions were clustered into families using a root mean square

Journal of PeptideScience

deviation (RMSD) criterion. Program PTRAJ from the AMBER package was employed for this type of clustering [28].Conformers showing best docking scores of each clustered family were promoted to MD simulation.

Molecular Dynamic Simulation of BChE Monomers

The protonation states of the ionizable residues were assumed as their ionization state at pH 7.0. Missing hydrogen and/or atoms were added according to the residue topology template. Crystallographic water molecules were retained in our model. The all-atom ff99SB force field [29] was selected to describe the complex in a periodic cubic TIP3P [30]explicit water box until 10 Å from the solute. Finally, the proper number of counter ions was added to proper neutralize the model.

MD equilibration and production: All MD simulations were carried out using the GPU implementation of the PMEMD program [31] in Amber 12 [32]. We followed a slight modification of the procedure published elsewhere [20]. To remove clashes, one two-step minimization was carried out to relax the water molecules (5000 steps), while the backbone atoms of the complex were constrained with 10 kcal/(mol $Å^2$) force constant. Then, whole system was allowed to relax for 5000 steps without any constraint. The relaxed geometry resulted in a backbone RMSD < 0.5 Å from the reference crystal structure. Then the system was heated up from 10 to 300 K gradually under the NVT (constant number (N), volume (V), and temperature (T)) ensemble for 500 ps. The equilibration continued for another 2 ns MD simulations under NPT (constant number (N), pressure (P), and temperature (T)) ensemble [33]. In this step, the temperature was controlled to 300 K by the Langevin thermostat method [34] with a collision frequency of 1.0 ps^{-1}. Finally, to improve the statistical sampling, teen independent simulation with length limited to 20 ns under the NVT ensemble was carried out, accounting for a total simulation length of 2 μs. Each individual simulation was started reading the final coordinates obtained from the equilibration phase but generating random initial velocities at the target temperature and assigning different random seeds. Long-range electrostatic interactions were treated by the particle mesh Ewald method [35]. Short-range non-bonded interactions were truncated with an 8 Å cutoff. All bonds involving hydrogen atoms were constrained by the SHAKE method [36]. A time step of 2 fs was used for the integration of the equations of motion. Others control parameters were left at its defaults values. The analysis was carried out collecting snapshots of the system in time intervals of 5 ps along the trajectories.

Cholinesterase Inhibition

Acetylthiocholine iodide (ATCl), AChE (from electric eel), S-butyrylthiocholine chloride, and 5,5-Dithio-bis(2-nitrobenzoic acid) (Ellman's reagent, DTNB) were purchased from Sigma–Aldrich (USA), and BChE was obtained from human serum.

In Vitro Cholinesterase Inhibition Assay

Cholinesterase enzyme inhibitory potential of the test samples was determined following Ellman's method with slight modifications. Briefly, test samples were prepared in phosphate buffer at the initial concentration of 400 μM. For AChE inhibitory assay, 50 μL of phosphate buffer (pH 7.5) was added to a 96 wells microplate followed by 50 μL of test samples and 50 μL of 0.25 units/mL AChE enzyme. After 30 min of incubation, 100 μL of a solution of 0.2 M DTNB and 0.24 M of ATCl was added into each well, and absorbance of the colored end product was measured using a Metrolab Microplate Spectrophotometer at 405 nm. Each test was conducted in triplicate.

For BChE inhibitory assay, the same procedures were applied as AChE except for the use of enzyme and substrate, which were BChE from human serum and S-butyrylthiocholine chloride, respectively.

Hemolytic Activity (HA)

Human erythrocytes were isolated from heparinized blood by centrifugation (1000 g for 10 min) after washing three times with saline solution. Erythrocyte solutions were prepared to a concentration of 0.4% (*v*/v) in isotonic saline solution.

Test tubes containing 200 μL of erythrocyte solution were incubated at 37°C for 60 min with 200 μL of peptide solution at concentrations ranging from 50 to 400 μM. After centrifugation at 1000 g for 5 min, the supernatant absorbance was measured at 405 nm. Lysis induced by 1% Triton X-100 was taken as 100%.

Results and Discussion

As the aim of this study was to improve the inhibitory activity of **P1-Hp-1971**, four analogs of different lengths of the central region of the peptide were synthesized. This region was selected according to the preliminary docking studies that indicated that the central region of **P1-Hp-1971** interacted with the active site of the enzyme. A blind docking study was performed for the peptide **P1-HP-1971**. This study showed that this peptide might bind to different parts of the active site, all of them close to the binding site of the catalytic triad (Figure S1 in Supporting Information). It is important to note that most of the binding forms of peptide **P1-HP-1971** have the main interactions with the hydrophobic pocket, through the sequence of amino acids that are part of the central zone (LPLGAGPAA). The blind docking study indicates that the form of union energetically preferred and with greater population is the one that is shown in the Figure S2. In this figure, it is possible to observe in yellow color the sequence that would be playing an important role for the union of this peptide. On the bases of these results, for peptides **7–21**; **5–21,** and **8–16,** this sequence was maintained, whereas in the case of the smallest peptide (**11–16**), the six amino acids of this sequence were maintained.

The synthesized sequences are shown in Table 1. All **P1-Hp-1971** analogs have a net positive charge between +1 and +4. The experimental molecular mass determined by MALDI-TOF mass spectrometry is also shown in this table.

In a previous work [21],it was demonstrated that in H_2O, **P1-Hp-1971** did not show any preferential conformation, as expected for short linear peptides. In the presence of TFE spectra deconvolution suggested the contribution of 40% random conformation. In the presence of DPPG liposomes, **P1-Hp-1971** displayed 35–40% turn, and 40% have a random conformation. In the presence of DPPC liposomes, **P1-Hp-1971** was unordered.

The first step of our study was to conduct a study of docking for the four new peptide structures (**7–21, 5–21, 8–16,** and **11–16**) on the BChE protein model (pdb-1P0M). For this study, we use the HADDOCK web server and MD simulations. This exploratory study indicated that **P1-Hp-1971** could bind in a region near the site called gorge, indicating that this peptide could have some inhibitory effect on the enzyme. Molecular docking analysis and MD simulations were performed to acquire better insight into the mechanism of action of this peptide. The active site of both

enzymes (BChE and AChE) is located at the base of ~20 Å deep and narrow gorge from the surface of the enzyme and is composed by two subsites: (1) catalytic esteratic site (CES) and (2) peripheral anionic site (PAS) [1,18]. The catalytic triad residues are S198, H438, and E325 (BChE residue numbering). The active site consists of D70, Q71, S72, F73, P74, G75, F76, P281, Y282, G283, T284, P285, and L286 [2,3].

The docking analysis and MD simulations reveal that **P1-Hp-1971** interacts with the receptor primarily because of hydrophobic and mild polar interactions, situated near to the peripheral anionic site at the entrance of the gorge with prominent interactions with N68, Q119, A277, V288, A328, F329, and Y332 (Figure 1). Based on these results of molecular modeling, we tested the inhibitory effect of **P1-Hp-1971** on BChE. This peptide showed a moderate but significant inhibitory effect. Figure 2 displays the inhibitory effect of **P1-Hp-1971** against BChE.

As it is shown in Figure 2, at 400 μM, **P1-Hp-1971** presents a 35% of inhibition of BChE, while at lower concentrations, it did not exceed the 15%. In order to achieve a peptide with higher activity and considering the premise that a small-size peptide is a better option for the purpose of finding a new leader structure, the sequence of **P1-Hp-1971** was reduced from 21 to 17 amino acids. Thus, in the next step of our study, we simulated the possible interaction of peptide **5–21**(region5–21) with the enzyme. For the molecular modeling study of peptide **5–21**, we performed exactly the same steps that had been made for **P1-Hp-1971**. The combined studies of docking and molecular dynamics simulations indicated that this peptide would bind in a very similar area to that of **P1-Hp-1971**, but in this case, peptide **5–21** could interact a little more with gorge area showing greater interactions with amino acids N68, A277, and Y332 (Figure 3). Furthermore, the calculations of binding energies (Table 2) obtained for the two clusters for peptide **5–21** have

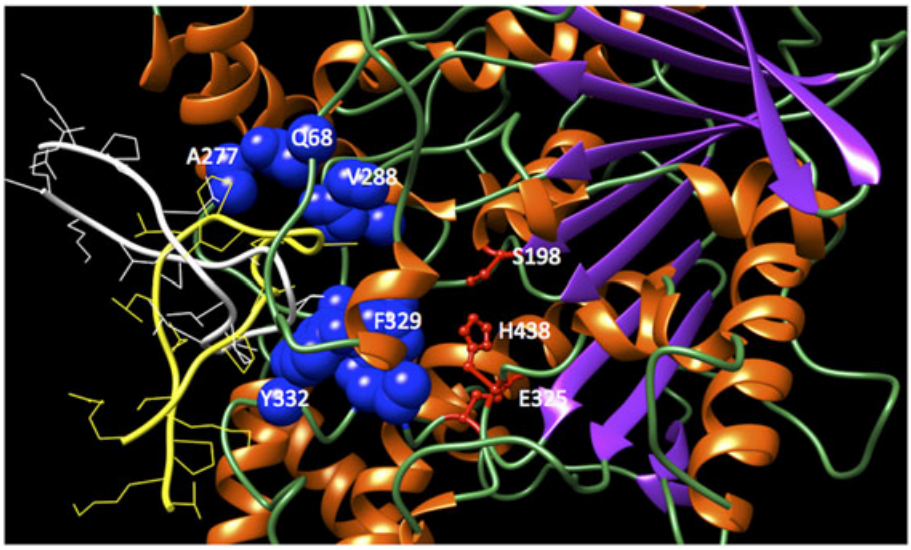

Figure 1. Spatial view of the two clusters (yellow and white) obtained **P1-Hp-1971** interacting in the active site of BChE. The names of the residues involved in the main interactions are written in the figure.

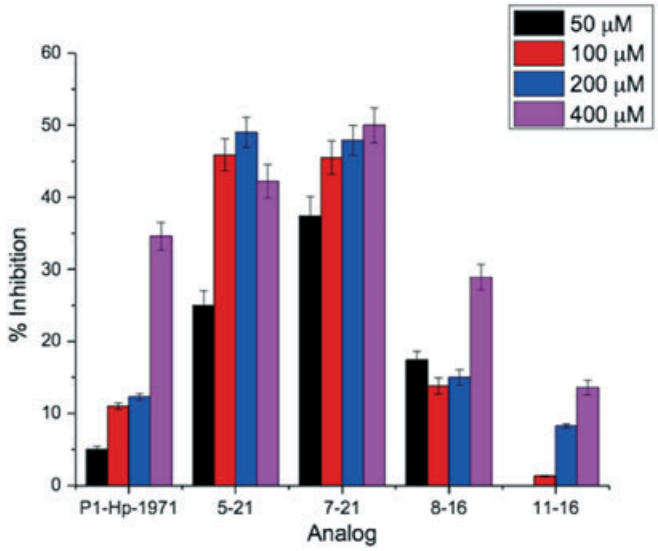

Figure 2. Percentage of BChE inhibition of the different synthetic peptides as a function of **P1-Hp-1971** analogs concentrations.

Journal of PeptideScience

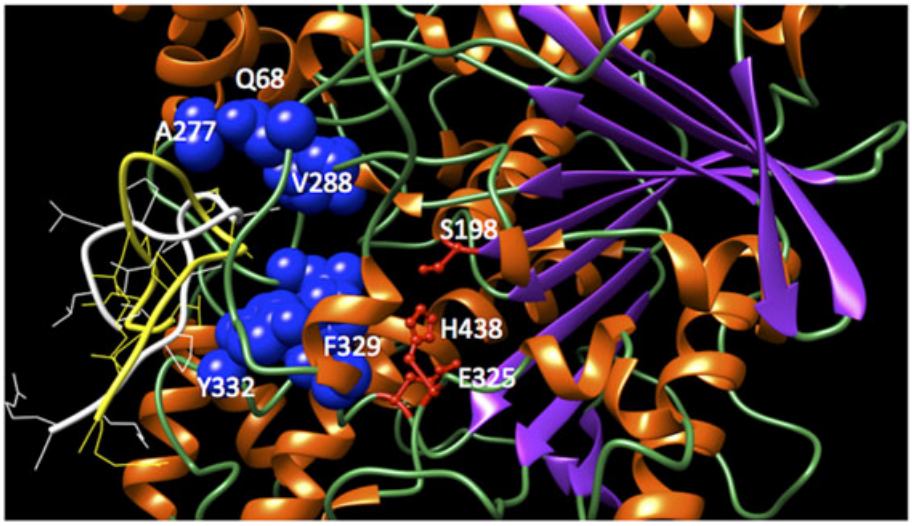

Figure 3. Spatial view of the two clusters (yellow and white) obtained peptide **5–21** interacting in the active site of Bache. The names of the residues involved in the main interactions are written in the figure.

Table 2. Relative free energy $G_{Binding}$ obtained in kcal/mol for the five complexes and two cluster studied here

—	$G_{Binding}$	
Peptide	Cluster 1	Cluster 2
P1-Hp-1971	−36.32	−25.09
5–21	−33.65	−24,65
7–21	−48.82	−67.68
8–16	−40.22	−45.12
11–16	−26.55	−19.63

suggested that this peptide would have a greater affinity for the enzyme with respect to **P1-Hp-1971** (Table 1). Based on these results, we decide to synthesize peptide **5–21** and test their possible inhibitory effect. The synthesis of this peptide is reported in the Materials and Methods section, and its inhibitory activity is shown in Figure 2. Our experimental results show that the peptide **5–21** has a greater inhibitory effect compared with **P1-Hp-1971** reaching near to the 50% of inhibition of BChE at 100 μM, which is fully in accordance with the results predicted by the MD simulations.

The sequence of peptide **5–21** was shortened in order to obtain peptide **7–21**(region7–21), which possesses 15 amino acids. The study of molecular modeling predicts that this peptide is inserted deeper into the groove entrance of the active site of the enzyme allowing having more interactions with the amino acids of the gorge site. Interestingly, peptide **3** (obtained from two clusters, shown in yellow and white in Figure 4) shows a greater number of interactions with the amino acids of gorge site, particularly with N68, L286, F329, and Y332. In addition, the binding energies (Table 2) obtained for these complexes showed lower values with respect to those obtained for **P1-Hp-1971** and peptide **5–21**(region5–21), indicating that this peptide would have a greater affinity for the enzyme. On the basis of such results, we synthesized peptide **7–21,** and later, the inhibitory effect was measured. As it can

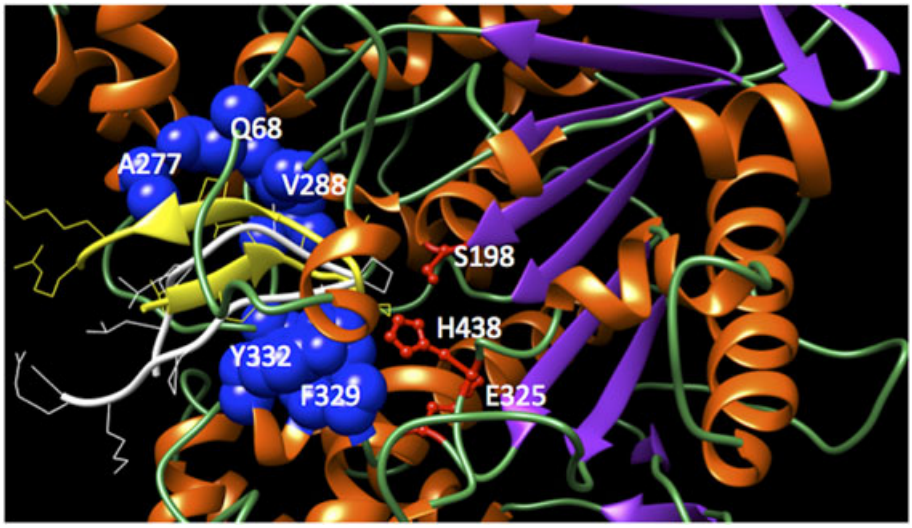

Figure 4. Spatial view of the two clusters (yellow and white) obtained peptide **7–21** interacting in the active site of Bache. The names of the residues involved in the main interactions are written in the figure.

be seen in Figure 2, this peptide displayed the highest inhibitory effect of this series (over than 50% of inhibition at the highest concentration), a result that is also in a complete agreement with the theoretical study.

The aforementioned results were very encouraging, and therefore, we were tempted to further shorten the sequence of peptide **7–21**. Thus, we simulated two new peptides, peptide **8–16** (region 8–16) and peptide **11–16** (region 11–16), which possess only nine and six amino acids, respectively, in their sequences (Table 1). The results obtained from the molecular modeling study for these two peptides showed marked differences with respect to those obtained earlier. While peptide **8–16** is located in a similar area of that of peptide **3,** and apparently it could have similar interactions with gorge site, it is interesting to note that the spatial ordering of the amino acid sequence of this peptide is completely different to those of the aforementioned peptides. Peptides **P1-Hp-1971**, **5–21,** and **7–21** interacts with the enzyme mainly with the central amino acids of the sequence, leaving the terminal amino acids (Table 1) practically outside the slit. In contrast, peptide **8–16** accommodates the terminal amino acids to interact with the enzyme leaving out of the active site the central amino acids (Figure 5). This is a substantial difference observed for this peptide with respect to its predecessors. Regarding the binding energies obtained for the two clusters obtained for peptide **8–16**, it should be noted that these values are higher than those obtained for peptide **7–21** indicating that peptide **8–16** could produce a lower interaction in comparison with peptide **7–21**; however, the values obtained for peptide **8–16** are comparable with those obtained for the peptide **5–21,** and therefore, we assumed that it would be interesting to synthesize and test this peptide. Peptide **11–16** is the smallest in this series, and it shows a completely different behavior from the rest of the peptides studied here. The results obtained from molecular modeling for peptide **11–16** indicate that this compound might be internalized deeply into the active site, even reaching the area near the catalytic site (Figure 6). At first, we take this result as a positive one regarding its possible inhibitory effect. However, the binding energy values obtained for this peptide were the highest of this series, indicating that this peptide would have the lesser affinity for the enzyme. At this stage of our study, we were a bit confused with these theoretical results so it was decided to seek an experimental corroboration, and therefore, in the next step, we decide to synthesize and to test peptides **8–16** and **11–16**.

The experimental results agree, at least qualitatively, with the results obtained for the binding energies of the different complexes. As we expected, peptide **11–16** only showed a relatively significant inhibitory effect (15%) to 400 μM, whereas at lower concentrations (200 and 100 μM), it showed just marginal activities, being totally inactive at 50 μM. With respect to compound **8–16**, this peptide showed an inhibitory effect markedly lower than those obtained for peptides **5–21** and **7–21**, but comparable with **P1-Hp-1971** (Figure 2). This result could be explained, at least in part, by the different conformational behavior observed for this peptide in comparison to those obtained for the more active peptides **5–21** and **7–21**.

Regarding a possible mechanism of action of these peptides at a molecular level, our results suggest that these compounds could act through an umbrella effect. There are many examples of inhibitors that do not bind to the binding site used by the natural chemical messenger. Such inhibitors are thought to bind to regions of the receptor that are close to the normal binding site. Although they do not bind to the binding site, the molecule acts as a 'shield' or as an 'umbrella' preventing the normal messenger from accessing the binding site. Our theoretical and experimental results allow us to think that this kind of mechanism might take place in this case.

At this stage of our work, and because dual inhibitors are of great importance in AD [7,12,37] , we wonder if these peptides also have an inhibiting effect on ACh. To answer that question, we performed the appropriate bioassays. Our results show that although these peptides also have inhibitory effects against ACh, this activity is

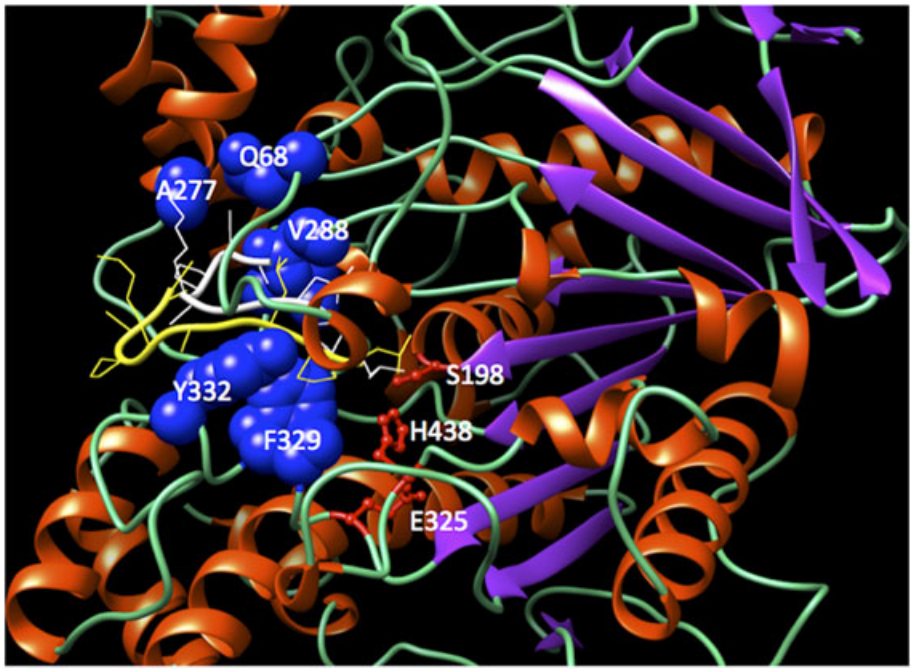

Figure 5. Spatial view of the two clusters (yellow and white) obtained peptide **8–16** interacting in the active site of Bache. The names of the residues involved in the main interactions are written in the figure.

Journal of PeptideScience

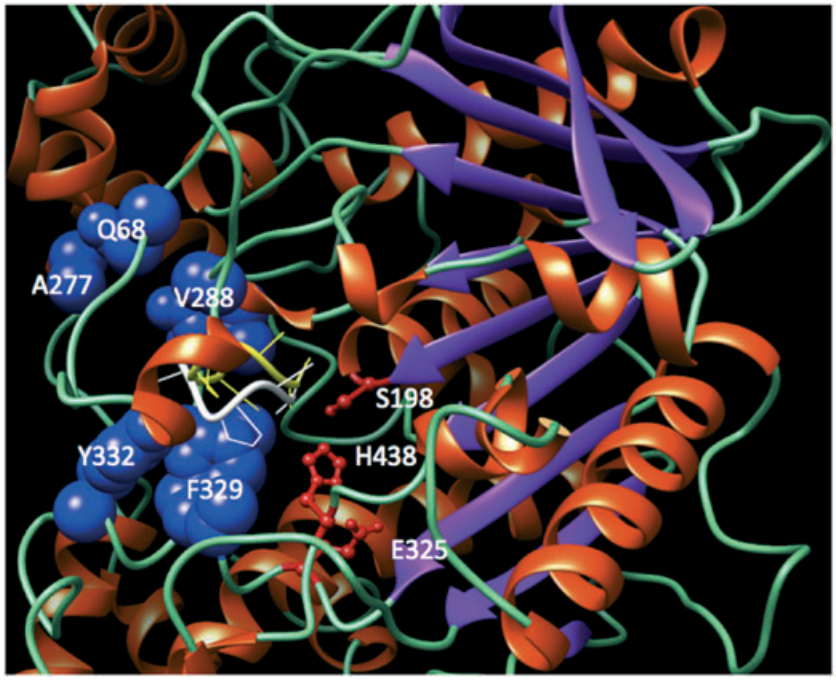

Figure 6. Spatial view of the two clusters (yellow and white) obtained peptide **11–16** interacting in the active site of Bache. The names of the residues involved in the main interactions are written in the figure.

significantly less potent than that observed for BChE (Figure 7). Peptides **5–21** and **7–21** showed the greater percent of inhibition of AChE, and peptides **8–16** and **5** inhibit in the same quantity than **P1-Hp-1971**. In this case, the longest analog, peptide **5–21**, was the one evidence of the greater percent of inhibition at 200 and 400 μM, achieving an inhibition greater than 50% (**P1-Hp-1971** shows an inhibition of 20% of the AChE). This result is not unexpected; after all, several theoretical and experimental results have been demonstrated that the different gating mechanisms due to the conformational dynamics of gating residues of AChE and BChE are responsible for their different substrate specificities.

Low hemolytic activity was found for all the analogs in the whole range of concentrations (50–200 μM). Peptide **5–21** was the most hemolytic of all and presents a 22% of hemolysis at 200 μM. Figure 8 depicts the percent hemolysis of human erythrocytes as a function of **P1-Hp-1971** analogs concentrations for the three peptides that show hemolytic activity. Peptides **8–16** and **11–16** evidence no hemolytic activity in the whole range.

It should be noted that the potential therapeutic use of these peptides in the AD is uncertain. However, the *in vitro* activity of these peptides (note that there are no previous reports of this activity for peptides) is interesting because they may represent new

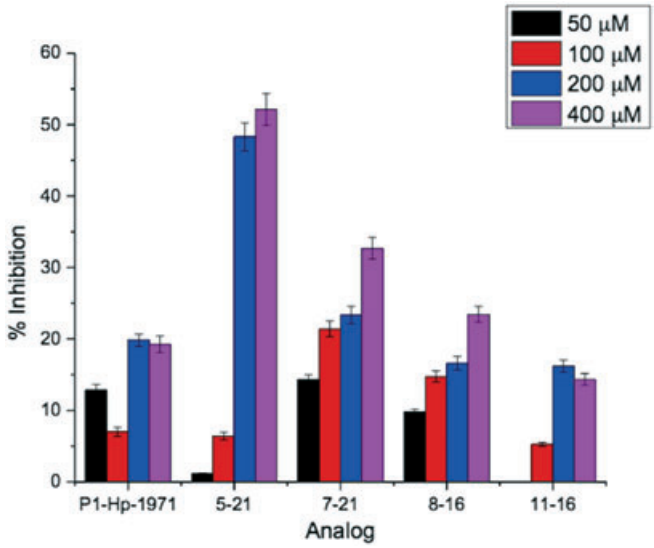

Figure 7. Percentage of AChE inhibition of the different synthetic peptides as a function of **P1-Hp-1971** analogs concentrations.

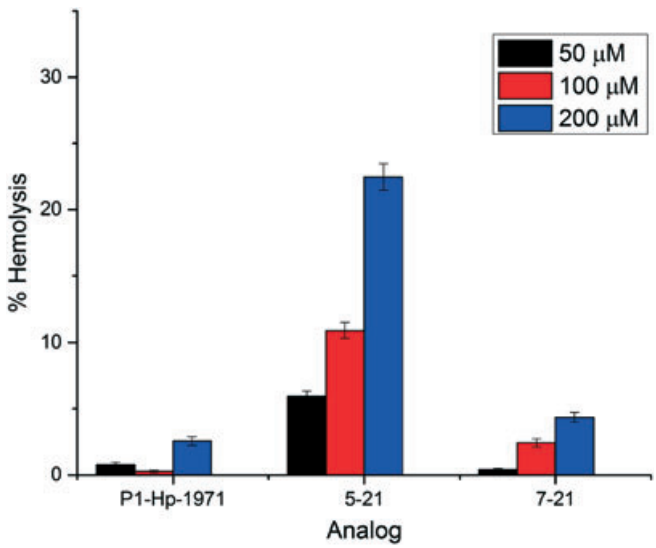

Figure 8. Percentage of hemolysis of human erythrocytes of the different synthetic peptides as a function of **P1-Hp-1971** analogs concentrations.

structural scaffolds (totally different from the currently known compounds) that can be used for the development of new inhibitors of this enzyme. Logically, these new compounds should be designed considering all pharmacokinetic aspects (which have not been considered in this study).

Conclusions

We report here for the first time peptide structures possessing inhibitory properties on BChE. It is important to note that these new peptides were designed from a study of molecular modeling. Thus, through the combined use of studies of docking and several simulations of molecular dynamics, it has been possible to design five new peptides with inhibitory activities on BChE. Among the peptides tested, peptide **7–21** showed the most significant inhibitory activity.

Although these peptides have only a moderate inhibitory effect, it is important to note that the mechanism of action at the molecular level by which these compounds produce inhibition seems to be particularly interesting. Our molecular modeling studies suggest that these peptides inhibit BChE by performing an umbrella-type effect, interacting at the gorge site next to the catalytic site of the enzyme. Based on our theoretical and experimental results, we believe that these peptides can be interesting starting structures for the design and development of new inhibitors of BChE.

In summary, we have described the molecular design, synthesis, and cholinesterase inhibition activities of five novel peptides. The bioassay data and cytotoxicity test show that some of compounds posses an inhibition that goes from 15% to 50% for both enzymes and no toxic effect. The present work demonstrates that diminution of the size of the original peptide could potentially result in new compounds with significant cholinesterase inhibition activity; although it appears that there is an optimal size for the sequence.

Acknowledgements

This work was supported by Universidad Nacional de San Luis (UNSL) and CONICET grants 2-1214 and PIP444, respectively. F. M. G, S. A. A., H. A. B., and R. D. E are staff members of the National Research Council of Argentina (CONICET, Argentina).The authors would like to thank MSc. Daniel O. Zamo for technical assistance (CONICET-Argentina).

References

1 Fuxreiter M, Warshel A. Origin of the catalytic power of acetylcholinesterase: computer simulation studies. *J. Am. Chem. Soc.* 1998; **120**: 183.
2 Boeck AT, Schopfer LM, Lockridge O. DNA sequence of butyrylcholinesterase from the rat: expression of the protein and characterization of the properties of rat butyrylcholinesterase. *Biochem. Pharmacol.* 2002; **63**: 2101.
3 Zhan CG, Gao D. Catalytic mechanism and energy barriers for butyrylcholinesterase-catalyzed hydrolysis of cocaine. *Biophys. J.* 2005; **89**: 3863.
4 Masson P, Froment MT, Gillon E, Nachon F, Lockridge O, Schopfer LM. Kinetic analysis of effector modulation of butyrylcholinesterase-catalysed hydrolysis of acetanilides and homologous esters. *FEBS J.* 2008; **275**: 2617.
5 Mesulam MM, Guillozet A, Shaw P, Levey A, Duysen EG, Lockridge O. Acetylcholinesterase knockouts establish central cholinergic pathways and can use butyrylcholinesterase to hydrolyze acetylcholine. *Neuroscience* 2002; **110**: 627.
6 Mesulam M, Guillozet A, Shaw P, Quinn B. Widely spread butyrylcholinesterase can hydrolyze acetylcholine in the normal and Alzheimer brain. *Neurobiol. Dis.* 2002; **9**: 88.
7 Giacobini E. Drugs that target cholinesterases.In *Cognitive Enhancing Drugs*, Buccafusco J (ed.). Birkhäuser Basel Switzerland, 2004; 11–36.
8 Berchtold NC, Cotman CW. Evolution in the conceptualization of dementia and Alzheimer's disease: Greco-Roman period to the 1960s. *Neurobiol. Aging* 1998; **19**: 173.
9 Shah RS, Lee HG, Xiongwei Z, Perry G, Smith MA, Castellani RJ. Current approaches in the treatment of Alzheimer's disease. *Biomed Pharmacother* 2008; **62**: 199.
10 Scarpini E, Scheltens P, Feldman H. Treatment of Alzheimer's disease: current status and new perspectives. *Lancet Neurol.* 2003; **2**: 539.
11 Karlsson D, Fallarero A, Brunhofer G, Mayer C, Prakash O, Mohan CG, Vuorela P, Erker T. The exploration of thienothiazines as selective butyrylcholinesterase inhibitors. *Eur. J. Pharm. Sci.* 2012; **47**: 190.
12 Musial A, Bajda M, Malawska B. Recent developments in cholinesterases inhibitors for Alzheimer's disease treatment. *Curr. Med. Chem.* 2007; **14**: 2654.
13 Ouberai M, Dumy P, Chierici S, Garcia J. Synthesis and biological evaluation of clicked curcumin and clicked KLVFFA conjugates as inhibitors of beta-amyloid fibril formation. *Bioconjug. Chem.* 2009; **20**: 2123.
14 Karlsson E, Mbugua PM, Rodriguez-Ithurralde D. Fasciculins, anticholinesterase toxins from the venom of the green mamba *Dendroaspis angusticeps*. *J. Physiol. Paris* 1984; **79**: 232.
15 Rodriguez-Ithurralde D, Silveira R, Barbeito L, Dajas F. Fasciculin, a powerful anticholinesterase polypeptide from *Dendroaspis angusticeps* venom. *Neurochem. Int.* 1983; **5**: 267.
16 Heath ML. Donepezil and succinylcholine. *Anaesthesia* 2003; **58**: 202.
17 Heath ML. Donepezil, Alzheimer's disease and suxamethonium. *Anaesthesia* 1997; **52**: 1018.
18 Greig NH, Lahiri DK, Sambamurti K. Butyrylcholinesterase: an important new target in Alzheimer's disease therapy. *Int. Psychogeriatr.* 2002; **14**(Suppl 1): 77.
19 Baruah J, Easby J, Kessell G. Effects of acetylcholinesterase inhibitor therapy for Alzheimer's disease on neuromuscular block. *Br. J. Anaesth.* 2008; **100**: 420.
20 Ortiz JE, Pigni NB, Andujar SA, Roitman G, Suvire FD, Enriz RD, Tapia A, Bastida J, Feresin GE. Alkaloids from *Hippeastrum argentinum* and their cholinesterase-inhibitory activities: an *in vitro* and *in silico* study. *J. Nat. Prod.* 2016; **79**: 1241.
21 Siano A, Humpola MV, de Oliveira E, Albericio F, Simonetta AC, Lajmanovich R, Tonarelli GG. Antimicrobial peptides from skin secretions of *Hypsiboas pulchellus* (Anura: Hylidae). *J. Nat. Prod.* 2014; **77**: 831.
22 Nicolet Y, Lockridge O, Masson P, Fontecilla-Camps JC, Nachon F. Crystal structure of human butyrylcholinesterase and of its complexes with substrate and products. *J. Biol. Chem.* 2003; **278**: 41141.
23 Nachon F, Nicolet Y, Viguie N, Masson P, Fontecilla-Camps JC, Lockridge O. Engineering of a monomeric and low-glycosylated form of human butyrylcholinesterase: expression, purification, characterization and crystallization. *Eur. J. Biochem.* 2002; **269**: 630.
24 Arnold K, Bordoli L, Kopp J, Schwede T. The SWISS-MODEL workspace: a web-based environment for protein structure homology modelling. *Bioinformatics* 2006; **22**: 195.
25 Biasini M, Bienert S, Waterhouse A, Arnold K, Studer G, Schmidt T, Kiefer F, Cassarino TG, Bertoni M, Bordoli L, Schwede T. SWISS-MODEL: modelling protein tertiary and quaternary structure using evolutionary information. *Nucleic Acids Res.* 2014; **42**: W252.
26 Bordoli L, Kiefer F, Arnold K, Benkert P, Battey J, Schwede T. Protein structure homology modeling using SWISS-MODEL workspace. *Nat. Protoc.* 2009; **4**: 1.
27 de Vries SJ, van Dijk AD, Krzeminski M, van Dijk M, Thureau A, Hsu V, Wassenaar T, Bonvin AM. HADDOCK versus HADDOCK: new features and performance of HADDOCK2.0 on the CAPRI targets. *Proteins* 2007; **69**: 726.
28 Case DA, Cheatham TE, 3rd, Darden T, Gohlke H, Luo R, Merz KM, Jr, Onufriev A, Simmerling C, Wang B, Woods RJ. The Amber biomolecular simulation programs. *J. Comput. Chem.* 2005; **26**: 1668.
29 Lindorff-Larsen K, Piana S, Palmo K, Maragakis P, Klepeis JL, Dror RO, Shaw DE. Improved side-chain torsion potentials for the Amber ff99SB protein force field. *Proteins: Structure, Function and Bioinformatics* 2010; **78**: 1950.
30 Jorgensen W, Chandrasekhar J, Madura J, Impey R, Klein M. Comparison of simple potential functions for simulating liquid water. *J. Chem. Phys.* 1983; **79**: 926.

31 Götz AW, Williamson MJ, Xu D, Poole D, Le Grand S, Walker RC. Routine microsecond molecular dynamics simulations with AMBER on GPUs. 1. generalized born. *J. Chem. Theory Comput.* 2012; **8**: 1542.
32 Case DA, Darden TA, Cheatham TE III, Simmerling CL, Wang J, Duke RE, Luo R, Walker RC, Zhang W, Merz KM, Roberts B, Hayik S, Roitberg A, Seabra G, Swails J, Götz AW, Kolossváry I, Wong KF, Paesani F, Vanicek J, Wolf RM, Liu J, Wu X, Brozell SR, Steinbrecher T, Gohlke H, Cai Q, Ye X, Wang J, Hsieh MJ, Cui G, Roe DR, Mathews DH, Seetin MG, Salomon-Ferrer R, Sagui C, Babin V, Luchko T, Gusarov S, Kovalenko A, Kollman PA. AMBER12 2012.
33 Berendsen HJC, Postma JPM, Gunsteren WFV, Dinola A, Haak JR. Molecular dynamics with coupling to an external bath 1984; **81**: 3684.
34 Lzaguirre JA, Catarello DP, Wozniak JM, Skeel RD. Langevin stabilization of molecular dynamics. *J. Chem. Phys.* 2001; **114**: 2090.
35 Essmann U, Perera L, Berkowitz M, Darden T, Lee H, Pedersen L. A smooth particle mesh Ewald method. *J. Chem. Phys.* 1995; **103**: 8577.
36 Ryckaert JP, Ciccotti G, Berendsen HJC. Numerical integration of the cartesian equations of motion of a system with constraints: molecular dynamics of n-alkanes. *J. Comput. Phys.* 1977; **23**: 327.
37 Khan I, Nisar M, Khan N, Saeed M, Nadeem S, ur Fazal R, Ali F, Karim N, Kaleem WA, Qayum M, Ahmad H, Khan IA. Structural insights to investigate Conypododiol as a dual cholinesterase inhibitor from Asparagus adscendens. *Fitoterapia* 2010; **81**: 1020.

Supporting information

Additional supporting information may be found in the online version of this article at the publisher's web site.

Molecular Design and Synthesis of Novel Peptides from Amphibians Skin Acting as Inhibitors of Cholinesterase Enzymes.
Figure 1S. Peptide P1-HP-1971 bind to different parts of the active site, all of them close to the binding site of the catalytic triad.
Figure 2S. Peptide P1-Hp-1971 (red) interacting in the active site. In yellow the LPLGAGPAA region is shown which was maintained in most of the synthesized peptides.

